PROCEEDINGS OF SCIENCE

Electron-argon scattering studies at Jefferson Lab

V. Pandey*
Center for Neutrino Physics, Virginia Tech, Blacksburg, Virginia 24061, USA
E-mail: vishvas.pandey@vt.edu

H. Dai, M. Murphy

Center for Neutrino Physics, Virginia Tech, Blacksburg, Virginia 24061, USA

D. Abrams

Department of Physics, University of Virginia, Charlottesville, Virginia 22904, USA

(For the Jefferson Lab Hall A E12-14-012 Collaboration)

For many decades, the study of electron scattering off a nucleus has been used as a tool to probe the properties of that nucleus and its electromagnetic response. In recent years, these studies have become vital starting point in the development of neutrino-nucleus scattering physics that constitutes largest share of systematic uncertainty in the accelerator-based neutrino-oscillation experiments. With the surge of Liquid Argon Time Projection Chambers (LArTPCs) based detectors in the short- (SBN) and long-baseline (DUNE) neutrino programs, the challenges of controlling systematics related to (anti)neutrino-argon scattering are magnified considering the isospin asymmetric nature of argon nucleus and the scarcity of electron-argon scattering studies. In light of these, an electron-argon experiment, E12-14-012, was designed at Jefferson Lab Hall A to study electron scattering on argon (N = 22) and titanium (Z = 22) nuclei using high precision continuous electron beam. The experiment collected data for $(e,e'p)$ and (e,e') processes on ^{40}Ar, ^{48}Ti and ^{12}C targets covering a broad range of energy transfers where quasielastic scattering and delta production are the dominant reaction mechanisms. In this contribution, we present a brief overview and status of the experiment.

The 20th International Workshop on Neutrinos (NuFact2018)
12-18 August 2018
Blacksburg, Virginia

*Speaker.

PoS(NuFACT2018)017

1. Introduction

In the last few decades, a number of electron-nucleus scattering experiments at different facilities around the world have provided wealth of information on the complexity of nuclear structure, dynamics and reaction mechanisms. The electron scattering off nuclei, governed by quantum electrodynamics, has advantage over the proton or pion scattering off nuclei which are dominated by strong forces. The electromagnetic interaction is well known within quantum electrodynamics and is weak compared to hadronic interaction and hence the interaction between the incident electron and the nucleus can be treated within the Born approximation, i.e. within a single-photon exchange mechanism. The ability to vary electron energy and scattering angle, hence the energy and moment transferred to the nucleus (ω, q), combined with the advancement in high-intensity electron beams, high performance spectrometers and detectors resulted into investigating specific processes ranging from quasielastic to Δ resonance to complete inelastic (resonant, non-resonant, and the deep inelastic scatterings) with great details. Decades of experimental work has provided sufficient testbed to assess and validate theoretical approximations and predictions that propelled the theoretical progress staged around nuclear ground state properties, correlations, form factors, nucleon-nucleon interactions, and nuclear many-body theories.

The electron-nucleus scattering, besides being immensely interesting in itself, turned out to be vital for precision goals of accelerator-based neutrino-oscillation experiments where the details of neutrino-nucleus scattering constitutes largest share of systematic uncertainty. To this end, the data collected with electron-nucleus scattering has provided the benchmark to test the nuclear models that can be further extended to neutrino-nucleus scattering. The vector currents probed in (unpolarized) electron scattering remain conserved between electron and neutrino scattering through conserved vector current (CVC) hypothesis. The extension of the formalism from electron-nucleus scattering to neutrino-nucleus scattering entail addition of the axial current contribution to the latter. Recently, with the surge of Liquid Argon Time Projection Chambers (LArTPCs) based detectors in the short- (SBN) [1] and long-baseline (DUNE) [2] neutrino program, the challenges of controlling systematics related to (anti)neutrino-argon scattering are magnified considering the isospin asymmetric nature of argon nucleus and scarcity of electron-argon scattering studies.

In light of these, we performed a dedicated electron-argon experiment at Jefferson lab Hall A [3]. We aim to measure spectral functions (SF) of the argon nucleus in the kinematic region in which shell-model dynamics is dominant, as well as to measure the (e, e') and $(e, e'p)$ cross sections on ^{40}Ar, ^{48}Ti, and ^{12}C nuclei. The choice of titanium nucleus (Z = 22) is driven by the fact that the neutron spectrum of argon (N = 22) is mirrored by the proton spectrum of titanium, hence the titanium data can be used to access the neutron spectral function of argon. These measurements will provide information on the energy and momentum distribution of protons and neutrons bound in argon and will allow an accurate reconstruction of the incident neutrino and antineutrino energy. Measuring SF of argon nucleus will provide a vital input in the further development of a unified nuclear model based on nuclear many-body theory and the spectral function formalism [4, 5, 6, 7]. Nevertheless, these new precise measurements will provide valuable testbed to the community and will pave the way to the development of theoretical models of electroweak interactions on argon nucleus in the kinematic region of interest to neutrino experiments.

2. E12-14-012 Experiment at Jefferson Lab Hall A

Experiment E12-14-012, performed in JLab Hall A during February-March 2017, collected high statistics $(e,e'p)$ data in five different kinematic configurations in which shell-model dynamics is dominant and collected (e,e') data in one kinematic configuration. The incoming electron beam energy, the scattered electron energy (and therefore the energy transfer) and the momentum of the knocked out proton are held fixed. Now, by varying the scattering angle (and moving the HRS accordingly), we spanned over different missing momentum to scan the kinematics region where shell model dynamics is known to dominate and single-particle aspects of the nuclear structure can be probed.

2.1 Coincidence $(e,e'p)$, and (e,e') Reactions

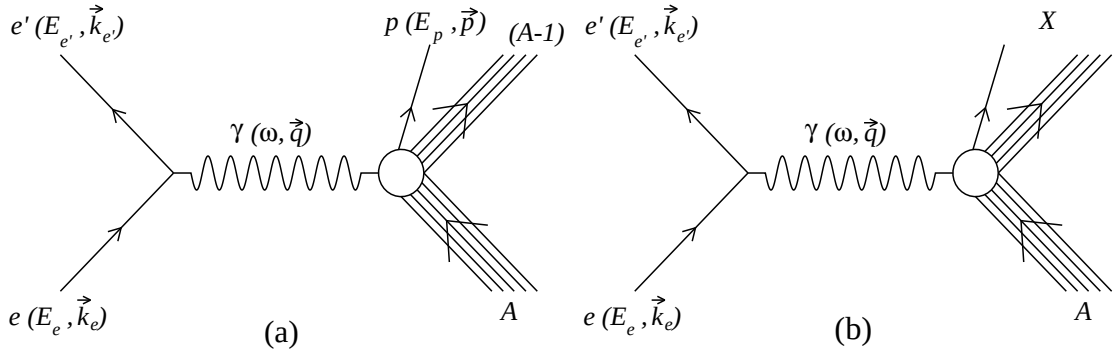

Figure 1: Processes considered in the E12-14-012 experiment: (a) Coincidence $(e,e'p)$ reaction where scattered electron and knocked out proton are measured in coincidence and the residual nucleus is left undetected, and (b) (e,e') reaction where only scattered electron is detected.

We considered coincidence $(e,e'p)$ process, as shown in Fig 1(a), where an electron of four-momentum $k_e \equiv (E_e,\vec{k}_e)$ scatters off a nuclear target A and knocks-out a proton of four-momentum $p \equiv (E_p,\vec{p})$, leaving the residual $(A-1)$ system in any (undetected) bound or continuum state

$$e + A \rightarrow e' + p + (A-1). \tag{2.1}$$

The knocked out proton is detected in coincidence with the scattered electron of four-momentum $k_{e'} \equiv (E_{e'},\vec{k}_{e'})$. The transferred four-momentum of the process is given as $q = k_e - k_{e'} \equiv (\omega,\vec{q})$. Such a reaction is a valuable source of information on the single-particle aspects of nuclear structure where one can define missing energy, E_m, from the energy conservation.

Within the Plane Wave Impulse Approximation (PWIA) scheme, i.e. on the assumptions that at momentum transfers $q \gg \frac{1}{d}$ where d is the average inter-nucleon distance, the scattering from the nucleus can be reduced to incoherent sum of scattering from individual nucleons and that the final state interaction (FSI) between the produced hadron and the residual nucleus are negligible, the missing momentum can be estimated as $\vec{p}_m = \vec{p} - \vec{q}$ and the missing energy, in the limit of low missing momentum, can be reduced to $E_m = \omega - T_p$, where $T_p = E_p - m$ is the kinetic energy of the outgoing proton. It is worth pointing out that despite PWIA scheme can provide a clear manifest of the description of the $(e,e'p)$ reaction, the corrections arising from the FSI between outgoing

nucleon and the residual nucleus are not negligible. These, for example, can be treated within the Distorted Wave Impulse Approximation (DWIA) description [8], and will be taken care of in the analysis of the $(e,e'p)$ data. The total SF, which describes the probability distribution of finding a nucleon with momentum p_m and removal energy E_m in the target ground state, can be expressed as

$$P(p_m,E_m) = P_{MF}(p_m,E_m) + P_{corr}(p_m,E_m). \tag{2.2}$$

Where the mean-field part of the SF, $P_{MF}(p_m,E_m)$, which corresponds to low missing momentum and energy region and hence where the shell model dynamics dominates, can be extracted from coincidence $(e,e'p)$ data. While correlation part of the SF, $P_{corr}(p_m,E_m)$, which corresponds to the ground state nucleon-nucleon (short-range) correlations, is evaluated from theoretical calculations of uniform nuclear matter and Local Density Approximation (LDA).

In the (e,e') process, as shown in Fig 1(b), an electron of four-momentum $k_e \equiv (E_e,\vec{k}_e)$ scatters off a nuclear target A

$$e + A \rightarrow e' + X \tag{2.3}$$

the energy and the scattering angle of the scattered electron are measured, while the hadronic final state is left undetected. Here, the cross section includes all available final states.

2.2 Measurement of (e,e') Cross Sections

We measured (e,e') cross sections on ^{12}C, ^{48}Ti [9] and ^{40}Ar [10, 11] at beam energy $E =$ 2.222 GeV and electron scattering angle $\theta = 15.541$ deg. The measurement of the carbon cross section allowed a comparison with previous experiments and is used to carefully study the systematic uncertainties. A continuous-wave electron beam of energy E = 2.222 GeV is provided by the Continuous Electron Beam Accelerator Facility (CEBAF) at JLab. The current and position of the beam is monitored by resonant radiofrequency cavities (Beam Current Monitors) and cavities with four antennae (Beam Position Monitors), respectively. The scattered electrons go through the Left High-Resolution Spectrometer (LHRS) positioned at $\theta = 15.541$ deg. In LHRS, the scattered electrons first pass through three superconducting quadrupole magnets and one dipole magnet that provide a large acceptance in both angle and momentum, and good resolution in momentum, position and in angle. The electrons then enter the detector package consists of a scintillator detectors, vertical drift chambers (VDCs) and threshold Čerenkov counter. The scintillator planes trigger the data-acquisition system, the particles are identified by a gas Čerenkov detector mounted between the two scintillator detector planes, and the tracking information (position and direction) is determined in VDCs [12].

First, the electron yield is determined as $Y^i = (N_S^i \times DAQ_{pre-scale})/(LT \times \varepsilon)$ where N_S^i is the number of scattered electrons, LT is the live-time fraction, ε is the total detection efficiency, and $DAQ_{pre-scale}$ determines what fraction of the events gets recorded. Then, the cross section is extracted either by the *acceptance-correction method* or by the *yield-ratio method*. In the acceptance-correction method, for each bin in $\Delta E \Delta\Omega$, the cross section is obtained as

$$d^2\sigma/d\Omega dE' = Y(E',\theta)/[(\Delta E \Delta\Omega)A(E',\theta)L] \tag{2.4}$$

with $Y(E',\theta)$ and $A(E',\theta)$ are yield and acceptance for a given bin, and L is the integrated luminosity. While, in the yield-ratio method, the cross section for each bin is computed as the product

of the Monte-Carlo cross section times the ratio of the data to simulation yields

$$d^2\sigma/d\Omega dE' = (d^2\sigma/d\Omega dE')_{MC} \times [Y(E',\theta)/Y_{MC}(E',\theta)]. \quad (2.5)$$

In our analysis presented in Ref. [10], we compared the cross sections obtained from both methods and found them in good agreement. Our measured cross sections of C(e,e') (within $<$ 3% total uncertainty), Ti(e,e') (within $<$ 3% total uncertainty) [9], and Ar(e,e') (within $<$ 4% total uncertainty) [10] cover a broad range of kinematics that includes quasielastic and delta-production peaks, and extends to the deep-inelastic scattering region. In Fig. 2 (obtained from Ref [9]), we compare the measured carbon and titanium cross section using the ratio $(d^2\sigma/d\Omega dE')/[Z\sigma_{ep} + (A-Z)\sigma_{en}]$ which shows differences in carbon and titanium cross sections due to different nuclear effects in these nuclei.

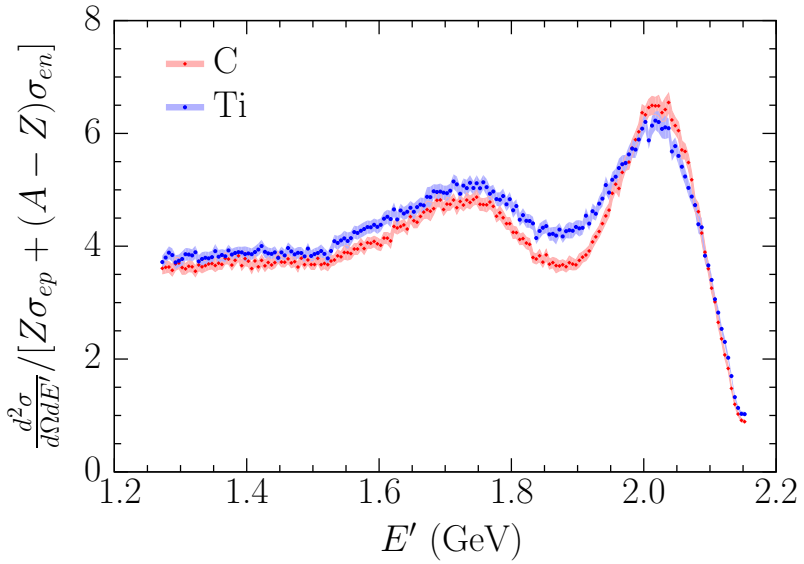

Figure 2: The figure from Ref. [9], shows the ratios $(d^2\sigma/d\Omega dE')/[Z\sigma_{ep}+(A-Z)\sigma_{en}]$ computed using the measured carbon and titanium cross section as a function of scattered electron energies.

3. Summary

The challenges of controlling systematic uncertainties related to (anti)neutrino-nucleus scattering, in liquid-argon based short- and long-baseline neutrino program, are magnified considering the isospin asymmetric nature of argon nucleus and scarcity of electron-argon scattering studies. In light of these, we performed a dedicated electron-argon experiment, E12-14-012, at Jefferson Lab Hall A to study electron scattering on argon (N = 22) and titanium (Z = 22) nuclei. We aim to measure the spectral function of argon nucleus, and (e,e') and $(e,e'p)$ cross sections. The high precision (e,e') cross sections are recently reported on carbon, titanium and argon nuclei covering a broad range of energy transfers where quasielastic scattering and delta production are the dominant reaction mechanism. These new precise measurements will be of great importance for the development of theoretical models of electroweak interactions on argon nucleus in the kinematic region of interest to neutrino experiments.

Acknowledgments

VP is grateful to the organizers of the workshop for the invitation and hospitality. This experiment was made possible by Virginia Tech, the National Science Foundation under CAREER grant No. PHY-1352106, and supported by the DOE Office of Science, Office of Nuclear Physics, contract DE-AC05-06OR23177, under which Jefferson Science Associates, LLC operates Jefferson Lab.

References

[1] M. Antonello *et al.* (MicroBooNE, LAr1-ND, and ICARUS-WA104 Collaborations), arXiv:1503.01520 [physics.ins-det].

[2] B. Abi *et al.* (DUNE Collaboration), arXiv:1807.10334 [physics.ins-det].

[3] O. Benhar *et al.* (The Jefferson Lab E12-14-012 Collaboration), arXiv:1406.4080 [nucl-ex].

[4] O. Benhar, N. Farina, H. Nakamura, M. Sakuda and R. Seki, Phys. Rev. D **72**, 053005 (2005).

[5] A. M. Ankowski, O. Benhar, M. Sakuda, Phys. Rev. D **91**, 054616 (2015).

[6] N. Rocco, A. Lovato, O. Benhar, Phys. Rev. Lett. **116**, 192501 (2016).

[7] E. Vagnoni, O. Benhar, and D. Meloni, Phys. Rev. Lett. **118**, 142502 (2017).

[8] S. Boffi, C. Giusti, and F. D. Pacati, Phys. Rep. **226**, 1 (1993).

[9] H. Dai *et al.* (Jefferson Lab Hall A Collaboration), Phys. Rev. C **98**, 014617 (2018).

[10] H. Dai *et al.* (Jefferson Lab Hall A Collaboration), arXiv:1810.10575 [nucl-ex].

[11] S. N. Santiesteban *et al.*, arXiv:1811.12167 [physics.ins-det].

[12] J. Alcorn *et al.*, Nucl. Instrum. Meth. A**522**, 294 (2004).